ADVANCED CONCEPTS IN FAST IGNITION AND THE RELEVANT DIAGNOSTICS

Hideaki Habara, Kathryn Lancaster, Chris Reason, Chris Aldis, Bill Lester, T. Craig Sangster* and Peter Norreys

1. INTRODUCTION

Recent developments in high power lasers have allowed the study of new regimes of laser-matter interactions relevant to astrophysics[1], nuclear physics[2], and fusion energy research[3, 4]. In the context of inertial fusion energy research, the 'fast ignitor' (FI) concept[5] was proposed in order to relax the strict symmetry requirements for the laser irradiation of the spherical target and to reduce the drive energy needed to achieve high densities and the formation of the spark. However, other problems have gradually become clear with this scheme. These are relevant to the temporal and spatial stability of the propagation of the additional heating source, for example the high-energy electron beam, due to losses and deflection[6] of the ultra-intense laser pulse in the surrounding plasma and the transport through a considerable length of a plasma[7]. Here we describe a new compression geometry that eliminates these problems utilizing the cone-guided compression scheme[8], or the so-called 'advanced fast ignitor'[9]. The attraction of this scheme is that it makes easy to access to fuel core without the temporal and spatial uncertainty. Using this scheme, colleagues from Japan and UK reported the first experimental results of fast heating of the compressed super-solid density matter using an ultra-intense short pulse laser and showed that efficient compression and heating are both possible simultaneously[9, 10]. This new approach provides a route to efficient fusion energy production.

It is also important for fast ignitor scheme to understand how to accelerate the electrons and ions using short-pulse intense laser pulses in the overdense plasma and also how the particles propagate into the super-critical plasma from the viewpoint of an additional heating source. Recently there have been many reports in both simulation and experiment that demonstrate a number of different acceleration mechanisms. Some of these suggest the acceleration strongly depend upon the laser and the plasma conditions such as the laser polarization, intensity and the density scale-length[11]. In particular, recent simulations predict that the energy of the accelerated ions suddenly increases with higher laser intensity and that the ion acceleration direction is changed from the longitudinal (or laser) direction to the transverse direction as plasma density scale-length is increased[12]. Therefore, measurement of the accelerated ion momentum distribution helps us to understand the laser-plasma interactions under various controlled conditions.

Hideaki Habara, Kathryn Lancaster, Chris J. Reason, Chris Aldis, Bill Lester and Peter A. Norreys, Rutherford Appleton Laboratory, Chilton, Didcot, Oxon, OX11 0QX, UK.
*T. Craig Sangster, LLE, Univ. of Rochester, 250 E, River Road, Rochester, NY, 14623-1299, USA.

Advanced Diagnostics for Magnetic and Inertial Fusion, Edited by Stott *et al.*
Kluwer Academic/Plenum Publishers, New York, 2002

Neutron spectroscopy is one of the most fascinating methods to investigate the accelerated ion distribution processes generated by ultra-intense laser-plasma interactions (using beam-fusion neutron spectroscopy) [13, 14]. For this purpose, we are re-constructing the multi-channel neutron spectrometer, LaNSA[15, 16]. The system records the timing when the neutrons are detected at each scintillator in the array. These timings are converted into neutron spectrum via the time-of-flight (TOF) method. Neutron energy spectra taken at several different directions can then be used to determine the momentum distribution of the accelerated ions by taking into account the Doppler shifts of neutron spectra from 2.45MeV for each viewing angle. In this paper, we discuss the re-commissioning of the LaNSA system and the future experiments that are planned for the RAL PW laser system.

2. NOVEL GEOMETRY OF FAST IGNITION SCHEME

The first question to address in guided compression is the effect of the high Z walls on the stability of the foil during the compression phase. To study this interesting stability problem, an experiment was conducted on the Nd:glass laser VULCAN[17] at the Rutherford Appleton Laboratory. The laser can be supplied sub-ns long pulse laser and sub-ps short pulse laser simultaneously. Figure 1 shows the first experimental layout. The short pulse beam was focused onto an aluminum plane with Bi coating to backlight the plasma into the v-groove of copper block. The short pulse beam was focused onto an aluminum plane with Bi coating to backlight the plasma into the v-groove of copper block.

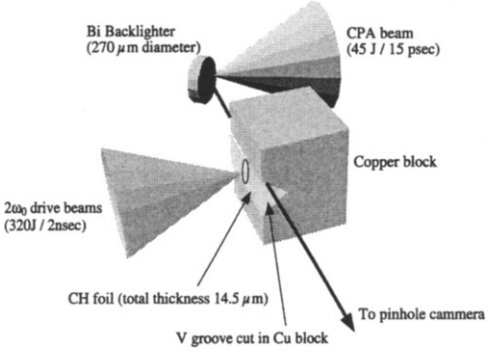

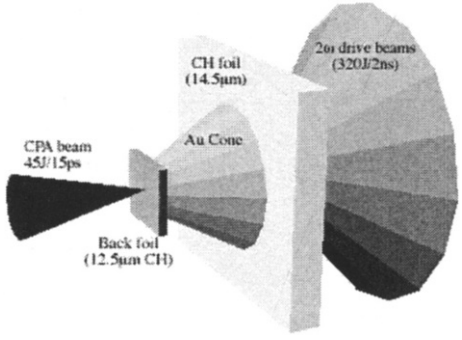

Left: **Figure 1**. Schematic illustration of the back-lighting experiment. Right: **Figure 2**.Schmatic illustration of conical implosion experiment.

The short pulse beam was focused onto an aluminum plane with Bi coating to backlight the plasma into the v-groove of copper block. The incident angle of the beam is 30 degree at peak intensity of 5×10^{14} W/cm^2. The 2ω drive beams were focused 500μm on the foil from the edge of the Cu block. The backlighting images were recorded with x-ray pinhole camera. In the results, we obtained an image of the guided plasma taken 1.0ns from the leading edge of the 2ns/5×10^{14}W/cm^2 pulse. The foil image shows some inner curvature at the edges of the v-groove without exhibition of the growth of any hydrodynamics instability at the foil surface.

A fully integrated conical compression experiment was conducted to determine the efficiency of fast electron heating. In this second experiment, the six 2ω nsec-duration beams irradiated a 12.5μm flat polyethylene CH foil, which was covered with a 2.0 μm of deuterated polystyrene CD foil as shown in Fig.2. A 100 μm diameter, 100nm thick signature layer of Ti and a 500nm thick layer of chlorinated paralyene were deposited between the CH and CD foils, with the CD layer facing the apex of the Au cone. The distance from the entrance hole to the apex was 250 μm and the Au cone material was 20 μm thick. A 20 μm hole was machined in apex of the cone, so that the target could be precisely positioned and the fast electrons transport was through the compressed CH/CD material only. A 12.5 μm thick, 270 μm diameter polyethylene foil was placed over the apex of the cone in order to control the scale-length of the short pulse interaction process. The p-polarized 45J/15ps pulse was focused onto this foil in a 20μm spot, giving a peak intensity on target of 10^{18}W/cm^2.

A significant increase in x-ray emission that peaked at 1.7ns after the beginning of the main pulse, corresponding to the onset of stagnation, was observed with the time resolved x-ray spectrometer. The time-integrated spectra indicated an upper bound to the heated plasma electron temperature of 1keV. Neutrons generated through DD thermal reactions were only observed at the same time of the peak of the X-ray emission, of which yield was 2×10^4 neutrons. Assuming the ρR of the plasma is 10mg/cm^2 from the simulations of the experiment, the plasma temperature will be estimated at 500eV, which agree with the result from X-ray spectroscopy. These results indicate that about 7% of the short pulse laser energy was coupled to the plasma to produce this temperature. While this coupling efficiency appeared somewhat low, it could be increased by a more suitable match of the range of the fast electrons to the achieved ρR. These experiments at RAL suggested that the high densities predicted by 2D computer simulations for the cone insert geometry could be achieved in practice.

The cone-guided compression experiments on heating of super-solid density plasmas were performed on the GEKKO XIII laser at the University of Osaka. This laser has 12 beams for nanosecond pulses with a maximum energy of 15kJ at 0.53μm wavelength and a synchronized sub-ps pulse beam with a power of 100TW and pulse energy of 60J[18]. The schematic diagram for the experiment is shown in Figure 3. Long pulse lasers irradiate the spherical target excepted with the area where the cone is inserted. At the proper timing of the implosion, ultra-intense laser is focused on the imploded core guided the propagation path free from the disturbance by an expansion and implosion of the plasma. The distance between the cone apex and center of the shell is 50μm, which is enough short to access to the core fuel with reduction of the sensitivity to electron beam propagation instabilities and losses. The cone walls are on a radius from the shell centre in order to minimize the disruptions to the spherical symmetry at the implosion and achieve high density. The laser energy of the drive pulses was 1.2kJ to measure the core heating taking account of the internal energy of the compressed core (about 5% of drive energy) to be comparable to the short pulse laser energy. The imploded core was observed at the center of the shell, which is estimated 40-45μm from X-ray self-emission image of the compressed plasma.

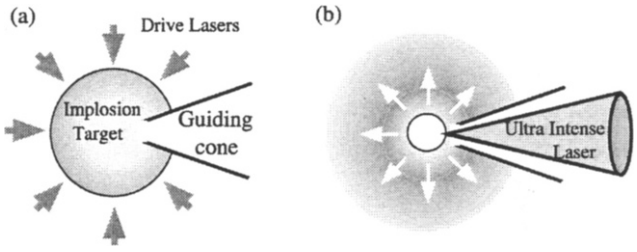

Figure 3. Schematic illustration of the cone-guided implosion. (a)Drive lasers irradiate the spherical target with a cone. (b) Ignition via additional heating by the fast electrons generated by the ultra-intense laser, which is propagated into the cone instead of the plasma channel.

The compressed core area is observed without short pulse injection, resulting in elliptical shape of $40 \times 25 \mu m^2$. The sequences of images of the core emission with and without the heating pulse were also taken with an X-ray flaming camera. The sequence when the short pulse is injected after the maximum compression of the shell clearly indicates the re-heating of the core by the short pulse after the brightness due to the compression is decreased. The size of the emission region at the peak of compression is about 30μm and increases to 50μm due to the injection of the heating pulse. These results coincide with the independent measurement of the heating region using the Al block.

Heating of the highly compressed plasma was measured through neutron spectroscopy for 2.45MeV thermonuclear DD neutrons. The neutron energy spectra were obtained using time-of-flight scintillator/photomultiplier detectors from two different angles[19]. Peak at 2.45MeV energy on the spectra is observed when the heating pulse was injected at maximum compression timing corresponding to a thermonuclear neutron yield of $2 \pm 1 \times 10^5$ neutrons. This neutron yield was more than 10 times above the numbers ($9 \pm 1 \times 10^3$) without or delayed injection of the short pulse. The efficiency of the energy coupling of the energetic electrons to the highly compressed plasma was estimated from the neutron yield and the heated volume inferred from the x-ray images. The heated mass is estimated from the density (50-70g/cc), the volume estimated by X-ray emission ($25 \times 40 \times 40 \mu m^3$). In order to increase the neutron yield by a factor of 10, a temperature at the region has to increase about 120eV (+/-20%) from the initial temperature regions of several hundred eV, which corresponds to 12-16J of the energetic electrons derived from the ultra-intense laser-matter interaction experiment using a plane target. The total coupling efficiency of the short pulse laser to the core could therefore be 20-27% with the estimation errors of 8% from the uncertainness of the temperature and the heated volume. This is a very encouraging result for the first demonstration of short pulse laser heating. In future experiments, we plan to increase the short pulse laser energy to see if the conversion efficiency remains high using the PW lasers at RAL and Osaka University. We also plan to measure the growth of any Kelvin-Helmholtz instability that develops on the edge of the cone that could mix high Z material into the compressed core plasma by placing suitable H-like and He-like emitting layer there and measuring them by X-ray spectroscopy.

3. NEUTRON SPECTROSCOPY IN ULTLA-INTENSE LASER-MATTER INTERACTIONS

We are also planning multi-channel neutron spectroscopy to measure the momentum distribution of accelerated ions inside the target. One possible way of measuring the ion momentum distribution is by direct observation of ions with plastic nuclear track detectors such as a CR-39. However, the ion motion is likely to be strongly affected by a large electric and/or magnetic fields in the plasma. Neutron spectroscopy, on the other hand, has the advantage that neither the target potential nor the self-generated magnetic fields can affect the motion of neutrons generated in the target. Unfortunately, the measurement of the neutron spectrum from just one direction does not give us the three-dimensional ion momentum distribution. It is necessary to measure the neutron spectra from at least two different directions to obtain the ion momentum distribution in the target.

Figure 4 (a) shows an example of neutron spectra generated by beam-fusion nuclear reactions from three different viewing angles[14]. The s-polarized, 1μm laser light was obliquely incident onto a CD 5μm target from 40 degree from target normal at an intensity of 10^{19}W/cm^2. The solid lines in all figures show the observed neutron spectra. Figure 4(a) shows experimental spectra at three observation angles: 90° or parallel to the target surface (solid line), 56° (dashed line) and 1° (dotted line) to the target normal, respectively. The peak of the spectra from the front side of the target shifts to lower energy (2.2MeV at 56°, 1.9MeV at 1°) from 2.45 MeV given by D-D thermal neutron energy while there is almost no shift in the spectra along the target surface direction (solid line). These shifts suggest that ions are accelerated into target inside taking account of the momentum conservation, which is similar to a Doppler effect on the neutron spectra. To investigate the precise momentum distribution of the ions, we performed 3D Monte-Carlo simulations to compare the calculated spectra with the experimental results. Figure 4(b) shows the well fitted calculated spectra at the same viewing angle as the experiments, which indicates that the ions are accelerated into the target, exactly opposite to the target normal direction. The ion distribution is shown in Fig.4(c) as a contour plot projected on the x-y plane from the 3-D distribution. The distribution collimated the target rear direction is given as a momentum ratio of P_x:P_y:P_z=2.3:1:1. The ion energy to the x-direction corresponding to the direction into the target is 330keV whereas the energy to the y and z-direction is about 70keV.

The neutron detector that we are re-constructing for the next generation experiments is the multi-channel spectrometer, LaNSA[15, 16], which originally consisted of 960 channels of scintillator-photo-multiplier detectors. In order to measure the neutron angular distribution, these modules will be divided into three separate units, each of which has 240 channels. The neutron detectors consist of an array of Thorn-EMI9902KB05 photo-multipliers coupled to BC505 liquid scintillator. The electrical signals are delivered to a Time-Digital-Converter (TDC), which records the arrival time of the signal via a discriminator. These timings are collected and then converted into a neutron spectrum through the time-of-flight (TOF) method. The data acquisition of the system is based on PC to control all CAMAC and Fastbus modules.

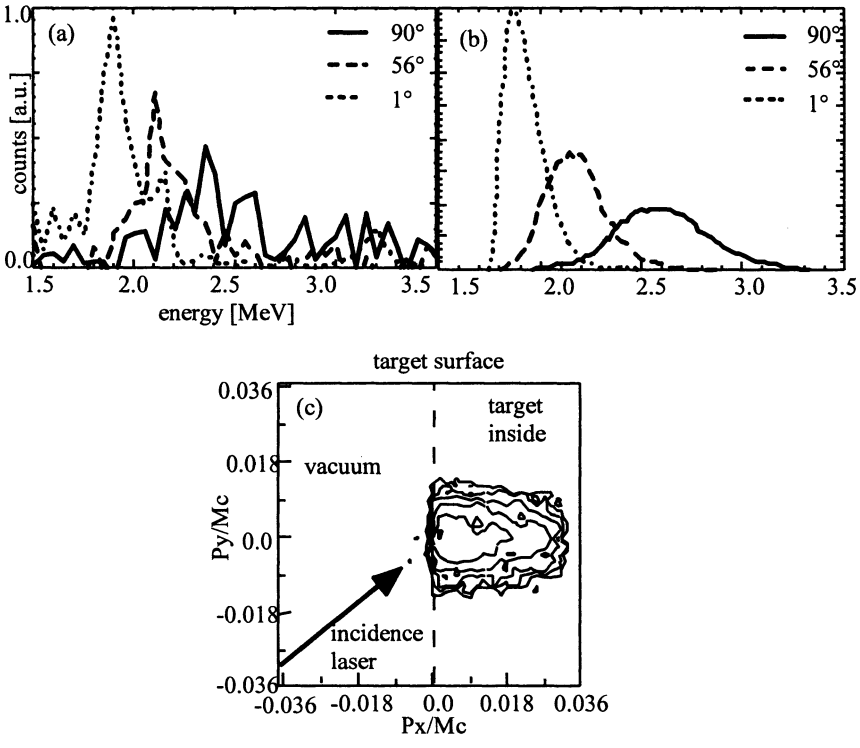

Figure 4. An example of (a) neutron spectra, (b) well-fitted calculated spectra and (c) the well-fitted ion momentum distribution[14].

These three modules will be positioned in target area PetaWatt (TAP) and target area west (TAW) of the VULCAN laser facility at the Rutherford Appleton Laboratory. Figure 5 shows an schematic image of the neutron array for one spectrometer in TAP together with an overview of the setup for PW laser and the neutron spectrometers. An image of chamber and the module at TAW is also shown in Fig.6. The neutron detector modules are represented by yellow box and the neutron flow is given by green gimlet area in both images. The distance between the two modules and the chamber center in TAP is about 12m and 5m. The distance of the array in TAW is about 8m from the chamber center.

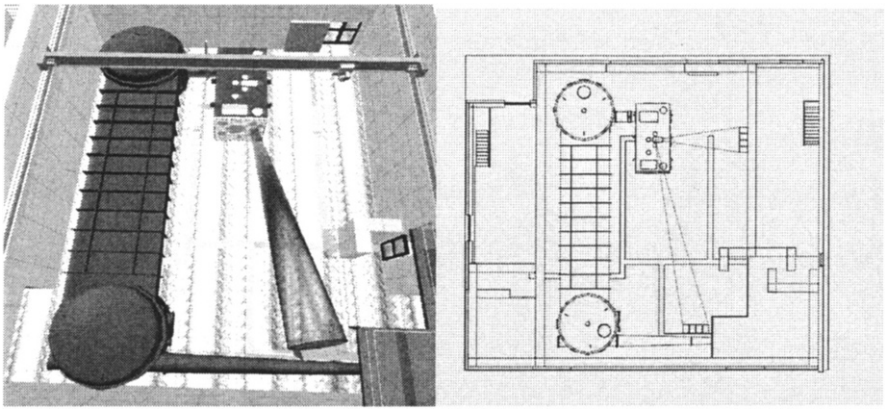

Figure 5. Image for one module at PW laser chamber room (TAP) and overview of PW laser and the neutron spectrometers.

The energy resolution for each module as a function of distance from the target is shown in Fig.7 for different neutron energies. The shorter the distance between the spectrometer and the focal position, the worse the energy resolution of the neutron spectrum becomes. For example, at 5m distance, the module has 300keV of energy resolution for 2.45MeV neutrons, whereas there is only 800keV resolution for 14MeV neutrons. On the other hand, at 12m distances, the energy resolution of the module becomes much smaller (100keV for 2.45MeV neutron and 350keV for 14MeV neutron). Therefore, the module that is nearest the target will be set up so that it views an angle that is perpendicular to the expected ion acceleration direction. By adjusting the target rotation and the incident laser direction, the energy resolution of both modules can remain at a comparably low level. On the other hand, the dynamic range to detect the neutrons can be set by adjusting the voltage of the photo-multipliers and the discriminator threshold.

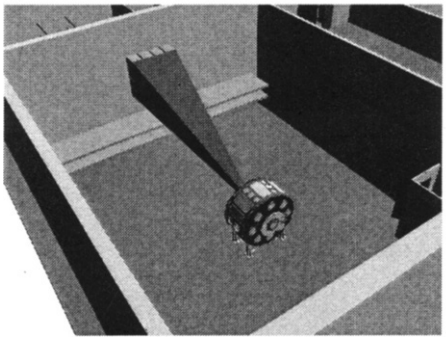

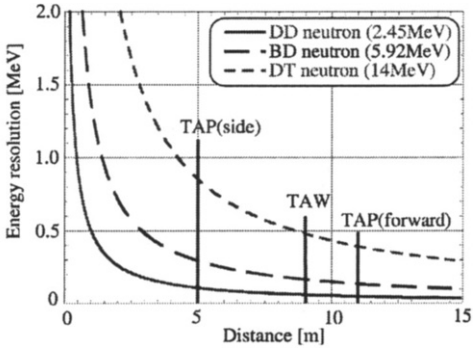

Left: **Figure 6**. Image of neutron detection at TAW. Right: **Figure 7**. Energy resolution for different neutron energy as a function of the distance between the spectrometer and laser focal position.

Using these neutron spectrometers, we plan experiments to measure the ion acceleration distribution for incident intensities up to 10^{21} Wcm^{-2}. It will be possible to change plasma density to determine the effect of scale-length on the ion acceleration

mechanisms. Measurement of neutron spectra generated by a number of different nuclear fusion reactions has other interesting applications. In particular, B-D and Li-D reactions generate higher energy neutrons and have higher energy cross sections than those of the DD reaction - this may lead to the simultaneous observation of the high energy part of the ion momentum distribution.

ACKNOWLEDGEMENTS

The work is supported by the UK Engineering and Physical Science Research Council. The LaNSA array is on loan from the U.S. Department of Energy to the UK Ministry of Defense.

REFERENCES

1. B. A. Remington, D. Arnet, R. P. Drake, and H. Takabe, Modeling astrophysical phenomena in the laboratory with intense lasers, *Science* **284**, 1488-1493.
2. E. P. Liang, S. C. Wilks, and M. Tabak, Pair production by ultraintense lasers, *Phys. Rev. Lett.* **81**, 4887-4890 (1998).
3. J. Nuckolls, L. Wood, Z. Thiessen, and G. Zimmerman, Laser compression of matter to super-high densities, *Nature* **239**, 139-142 (1972).
4. J. Lindl, R. L. McCrory, and E. M. Campbell, Progress toward ignition and burn propagation in inertial confinement fusion, *Phys. Today* **45**, 32-40 (1992).
5. M. Tabak et al., Ignition and high gain with ultra powerful lasers, *Phys. Plasmas* **1**, 1626-1634 (1994).
6. B. J. Duda, R. G. Hemker, K. C. Tzeng, and W. B. Mori, A long-wavelength hosing instability in laser-plasma interactions. *Phys. Rev. Lett.* **83**: 1978-1981 (1999).
7. S. Hain, F. Cornolti, and H. Opower, Hydrodynamic models and schemes for fast ignition. *Laser and Part. Beams* **17**, 245-263 (1999).
8. S. Hatchett and M. Tabak, presented at the anomalous absorption conference, ocean city, May 2000, (unpublished).
9. P. A. Norreys et al., Experimental studies of the advanced fast ignitor scheme, *Phys. Plasmas* **7**, 3721-3726 (2000).
10. R. Kodama et al., Fast heating of ultrahigh-density plasma as a step towards laser fusion ignition, *Nature* **412**, 798-802 (2001).
11. M. I. K. Santala et al., Effect of the plasma density scale length on the direction of fast electrons in relativistic laser-solid interactions, *Phys. Rev. Lett.* **84**, 1459-1462 (2000).
12. C. Toupin, E. Levebvre, and G. Bonnaud, Neutron emission from a deuterated solid target irradiated by an ultraintense laser pulse, *Phys. of Plasmas* **8**, 1011-1021 (2001).
13. P. A. Norreys et al., Neutron production from picosecond laser irradiation of deuterated targets at intensities 10^{19} Wcm^{-2}, *Plasma Phys. Control. Fusion* **40**, 175 (1998)
14. H. Habara et al., in: *High-Power Lasers in Energy Engineering*, edited by K. Mima, G. L. Kulcinski, and W. Hogan, (Proceedings of SPIE Vol. 3886, 2000), pp. 513-520.
15. M. D. Cable, S. P. Hatchett, and M. B. Nelson, Neutron spectroscopy with a large neutron time-of-flight detector array (LaNSA), *Rev. Sci. Instrum.* **63**, 4823-4827 (1992).
16. M. B. Nelson and M. D. Cable, LaNSA:A large neutron scintillator array for neutron spectroscopy at NOVA, *Rev. Sci. Instrum.* **63**, 4874-4876 (1992).
17. C. N. Danson et al., Well characterized 10^{19} Wcm^{-2} operation on VULCAN – an ultra-high power Nd:glass laser, *J. Mod. Opt.* **45**, 1653-1669 (1998).
18. Y. Kato et al., Fast ignition and related plasma physics issues with high-intensity lasers. *Plasma Phys. Contril. Fusion* **39**, 145-151 (1997).
19. N. Izumi et al., A highly efficient neutron time-of-flight detector for inertial confinement fusion experiments, *Rev. Sci. Instrum.* **70**, 1221-1224 (1999).